




Article

Influence of the Nonequilibrium Material State on Wear Resistance

Iosif Gershman ^{1,2,*} , Alexander Mironov ^{1,2}, Stephen Veldhuis ³ , Eugeny I. Gershman ¹, Pavel Podrabinnik ¹  and Ekaterina Kuznetsova ¹

¹ Laboratory of Electric Currents Assisted Sintering Technologies, Moscow State University of Technology “STANKIN”, Vadkovsky Lane 3a, 127055 Moscow, Russia; lecast@stankin.ru (A.M.); dosbaem@mcmaster.ca (E.I.G.); p.podrabinnik@stankin.ru (P.P.); evkuznetsova1@gmail.com (E.K.)

² Department of Scientific Research Programs, Grants And Projects, Railway Research Institute JSC “VNIIZHT”, 3rd Mytischinskaya Street 10, 107996 Moscow, Russia

³ Department of Mechanical Engineering, McMaster University, 1280 Main Street West, Hamilton, ON L8S4L7, Canada; veldhu@mcmaster.ca

* Correspondence: isgershman@gmail.com; Tel.: +7-499-972-9494

Received: 4 June 2019; Accepted: 20 June 2019; Published: 23 June 2019



Abstract: The influence of the nonequilibrium state of a material on its wear resistance is investigated in this study. Using methods of non-equilibrium thermodynamics and the theory of self-organization, a non-equilibrium material is shown to possess an overall lower wear rate than a material in an equilibrium state. This was experimentally demonstrated to be the case in different materials and tribosystems, such as Babbitt operating in complete lubrication conditions, copper in the current collector and a cutting tool with a coating applied on it.

Keywords: friction; friction surface; secondary structures; self-organization; wear resistance

1. Introduction

Previous works concerning nonequilibrium thermodynamics and self-organization, characterize friction as a nonequilibrium process [1–5].

In [6–10] it is stated that materials enter a nonequilibrium state during friction due to the formation of secondary structures on the surface. In [2] the analyzed tribosystem deviated significantly from the equilibrium state. State analysis was based on the concept of reserved energy, the entropy of the system and entropy production. If energy delivered to the system has insufficient time to be dissipated by channels such as thermal conductivity, heterogeneous secondary structures that affect the state of the contacting surfaces are expected to manifest and grow in sliding bodies. Therefore, entropy might decrease, and the system will shift to a non-equilibrium state. According to [6], once secondary structures are formed, friction energy gets unevenly distributed within the rubbing body and becomes mostly concentrated in secondary structures.

As a consequence, the secondary structures perform protective functions, limiting the spread of interactions inside the rubbing bodies and reducing their intensity. Their appearance, therefore, corresponds to the Le Chatelier principle [11]. All other conditions being equal, increasing the degree of uneven distribution of energy within the rubbing body leads to a decrease in its entropy [12].

In a rubbing body, the friction energy is distributed according to a monotonically decreasing function with distance from the friction zone [6]. Conversely, the distribution of friction energy becomes abrupt as secondary structures form. Most of the friction energy is concentrated within the secondary structures, sharply decreasing at their boundary. This energy distribution has a greater degree of non-equilibrium compared to the case of a rubbing body where secondary structures are not present.

Under equal friction energies, the entropy of a friction body with secondary structures will be less than the entropy of a friction body without them. Thus, as the material reacts to friction, it will enter a non-equilibrium state. There are processes which strive to reduce entropy within the rubbing material, i.e., through negative entropy production. The material reacts to friction by dissociating from the equilibrium state, which leads to a decrease in the wear rate [13]. In this context, it becomes necessary to investigate the wear rate behavior of materials initially present in a state of non-equilibrium.

Theory

From [5,11], it follows that the wear rate decreases along with entropy production. In [11,13], it is noted that the production of entropy markedly decreases under tougher friction conditions due to self-organization and the formation of dissipative structures in the friction zone. Dissipative structures are characterized by processes with increased free energy and negative entropy production. The latter contributes to a decrease in the total entropy production of a friction body compared to its state under the same conditions without self-organization.

The entropy production of a rubbing body without self-organization is given in expression (1):

$$\frac{d_i S_1}{dt} = \sum \frac{d_i S_f}{dt} \quad (1)$$

where $\sum \frac{d_i S_f}{dt}$ is the sum of entropy production processes occurring in the rubbing body as a result of friction without self-organization. It should be noted that $\sum \frac{d_i S_f}{dt} > 0$.

The production of entropy after self-organization is given in (2):

$$\frac{d_i S_2}{dt} = \sum \frac{d_i S_f}{dt} - \left| \sum \frac{d_i S_s}{dt} \right| \quad (2)$$

where: $\frac{d_i S_2}{dt}$ is the production of the entropy in the rubbing body following self-organization; $\sum \frac{d_i S_s}{dt}$ is the sum of entropy production processes contributed by dissipative structures.

The second term on the right-hand side of (2) is expressed in terms of absolute value with a negative sign to emphasize the negative entropy production of dissipative structure processes.

Comparing (1) and (2) it can be concluded that:

$$\frac{d_i S_1}{dt} > \frac{d_i S_2}{dt} \quad (3)$$

Thus, according to [11], all other conditions being equal, the wear rate of the rubbing body during the course of self-organization is less than that of the rubbing body where self organization is absent.

From the point of view of thermodynamics, the nonequilibrium state of a material is characterized by the relatively high value of internal energy and the relatively low value of entropy. Examples of such materials include hardened alloys as compared to quenched and annealed materials, alloys with a high value of internal stresses as compared to annealed materials and others. Relaxation processes occur in these materials during heating, which bring it closer to the equilibrium state. In quenched materials, such processes can be the decomposition of a supersaturated solid solution, a decrease of the density of vacancies or recrystallization, whereas in materials that have increased internal stresses, these processes include the movement of dislocations with increasing uniformity of distribution by volume. Different relaxation processes can proceed through various mechanisms. Increasing entropy and decreasing internal energy are common features of these processes. Relaxation processes are accompanied by positive entropy production.

During the course of relaxation processes under friction, the entropy production of the rubbing body will increase in both cases with (4) and without self-organization (5):

$$\frac{d_i S_1}{dt} = \sum \frac{d_i S_f}{dt} + \sum \frac{d_i S_r}{dt} - \left| \sum \frac{d_i S_s}{dt} \right| \quad (4)$$

$$\frac{d_i S_1}{dt} = \sum \frac{d_i S_f}{dt} + \sum \frac{d_i S_r}{dt} \quad (5)$$

where: $\frac{d_i S_r}{dt}$ are the entropy production relaxation processes.

Comparing (5) and (4) with (1) and (2) respectively, it can be concluded that entropy production increases during the passage of the relaxation processes. Therefore, an increase in the wear rate is anticipated.

However, it was noted in [14] that the probability of self-organization rises along with the increasing complexity of the system. In [15,16], the probability of self-organization and the formation of dissipative structures with regard to friction processes on the surface of a rubbing body is estimated depending on the number of thermodynamic flows interacting with the rubbing body. In (6), the probability of thermodynamic stability loss of a rubbing body is given, which is a prerequisite for the initiation of self-organization:

$$P = 1 - \frac{1}{2n} \quad (6)$$

where: P is the probability of loss of thermodynamic stability, n is the number of thermodynamic fluxes.

From (6) it follows that the probability of thermodynamic stability loss increases alongside the number of flows. Consequently, the probability of self-organization also increases.

During friction of relatively non-equilibrium materials, thermodynamic flows of matter, energy, dislocations and accompanying relaxation processes are added to the thermodynamic flows caused by friction. According to (6), this increases the probability of self-organization

In non-equilibrium materials, self-organization will take place under less severe friction conditions than in equilibrium materials. Given the same friction conditions, self-organization is unlikely to commence in equilibrium materials but may take place in non-equilibrium ones. Self-organization in non-equilibrium materials will reduce the wear rate several times compared to relatively equilibrium materials without self-organization [13].

It should be noted that all previous arguments only apply if the properties of equilibrium and non-equilibrium materials are similar.

2. Materials and Methods

Three different tribosystems operating under different conditions were taken into consideration.

The first tribosystem simulated the friction process of a journal bearing and a steel shaft. Babbitt was chosen as the antifriction material (i.e., materials that have low friction coefficient, low ability for seizure), which are used in sliding bearings. Composition of Babbitt is shown in Table 1. This material is capable of natural aging at a temperature of 20 °C. Determination of properties and tribological tests of Babbitt were carried out after aging for one day, one month, six months and one year. Hardness, tensile strength, friction coefficient, score resistance and wear rate were evaluated.

Table 1. Composition of Babbitt shoe.

Elements Composition, % Weight				
Pb	Sn	Na	Ca	Mg
balance	2.01	0.3	0.14	0.033

The tribological tests were performed on the rotating steel roller–fixed shoe made of antifriction alloy (Figure 1). The analog of nickel-chromium steel SNC28 (Hakuro Group, Kasai, Japan) was used for roller production (Table 2). The radius of roller and shoe was 20 mm, and the width was 10 mm.

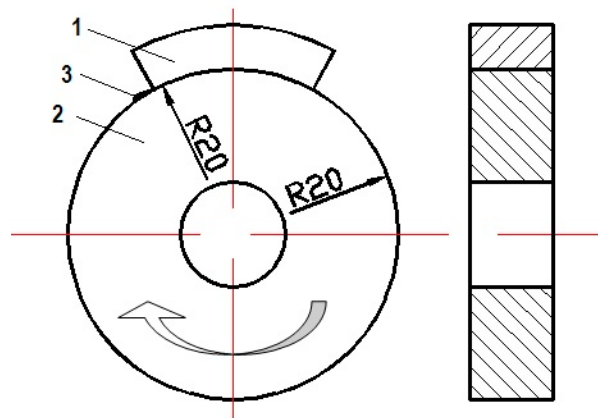


Figure 1. Kinematic configuration of the friction mechanism; 1—shoe, 2—roller, 3—lubricant.

Table 2. Composition of steel role.

Elements Composition, % Weight											
Main Components							Impurities				
Ni	Cr	Mn	Si	C	Mo	Fe	Cu	S	Al	V	Nb
2.81	0.681	0.625	0.295	0.35	0.477	94.42	0.087	0.011	0.018	0.185	0.013

The steel roller rotated at a speed of 500 r/min. An API CB group oil was used as a lubricant.

To evaluate the score resistance, the load increased step by step every 10 min by 50 N until a sharp (by several times) increase in the friction coefficient was reached. The wear of the steel roller and the Babbitt shoe were determined by the difference in mass before and after testing for 40 h under a load of 8 MPa.

Sliding electrical contacts are another tribosystem observed in this study. The test circuit was similar to that shown in Figure 1. The tests were performed in dry friction conditions. A lateral reciprocating movement of the shoe with a frequency of 200 displacements/min, and an amplitude of 10 mm was added to the rotation of the roller. The load was 245 N. An electric current of 40 A passed between the contacts. The roller was made of copper produced in a vacuum furnace. The cast billet was hot rolled. The copper was quenched in water at temperatures of 800, 850, and 900 °C. Quenched specimens were cold rolled with a degree of compression of 60%. The material properties of copper samples are shown in Table 3.

Table 3. Mechanical properties of copper specimens.

Quenching Temperature, °C	Hardness, HB	Tensile Strength, MPa	Electrical Conductivity, % IACS
800	111	358	97.8
850	112	361	97.3
900	112	362	97.0

The current collection material (shoe) was a sintered mixture of iron and copper powders. The sintered material was permeated with Pb-Sn alloys. The composition and properties of the alloys are provided in Tables 4 and 5 respectively.

Table 4. Composition of the current collection material.

Elements Composition, % weight			
Cu	Pb	Sn	Fe
8.4	17.2	1.1	balance

Table 5. Properties of the current collection material.

Hardness, HB	Electrical Resistivity, $\mu\Omega\cdot\text{m}$	Density, g/cm^3
160	0.28	7.3

Finally, behavior of the wear-resistant (TiAl)N coating on the cutting tool was studied. A conventional method of physical vapor deposition was used to coat the tool. The coating was also applied to the cutting tool by filtered arc deposition (FAD), which enabled finer coating grains to be obtained. A detailed description of the technologies and properties of the coatings deposited using the traditional equilibrium coating (PVD) method and FAD technology are given in [6,17]. The properties of the coatings are shown in Table 6. The milling speed was 240–450 m/min, cutting depth—0.5 mm. Steel 1040 was used as the workpiece.

Table 6. Properties of (TiAl)N coatings.

Coating	Chemical Composition, % Atom	Grain Size, nm	Coating Thickness, μm	Microhardness, GPa	Friction Coefficient
(TiAl)N PVD	Ti ₂₂ Al ₂₂ N ₅₆	50	3	33	0.986
(TiAl)N FAD	Ti ₂₂ Al ₂₂ N ₅₆	25	3	32	0.857

3. Results and Discussion

Table 7 shows the mechanical and tribological properties of Babbitt depending on the aging period.

Table 7. Mechanical and tribological properties of Babbitt depending on the aging period.

Properties	Aging Period			
	One Day	One Month	Six Months	One Year
Hardness, HB	20.4	25.0	26.7	28.7
Tensile strength, MPa	-	44.0	52.2	63.4
Friction coefficient	-	0.01	0.036	0.08
Scoring load, MPa	-	13.0	11.8	10.2
Wear rate, mg/40 h	-	0.0011	0.0025	0.0047

Table 8 shows wear rates of copper rollers quenched at different temperatures following friction with the current collector.

Table 8. Wear rates of copper rollers depending on quenching temperature.

Property	Quenching Temperature, °C		
	800	850	900
Wear Rate, mg/h	38.1	32.6	25.9

Figure 2 demonstrates the dependence of coating wear on cutting length.

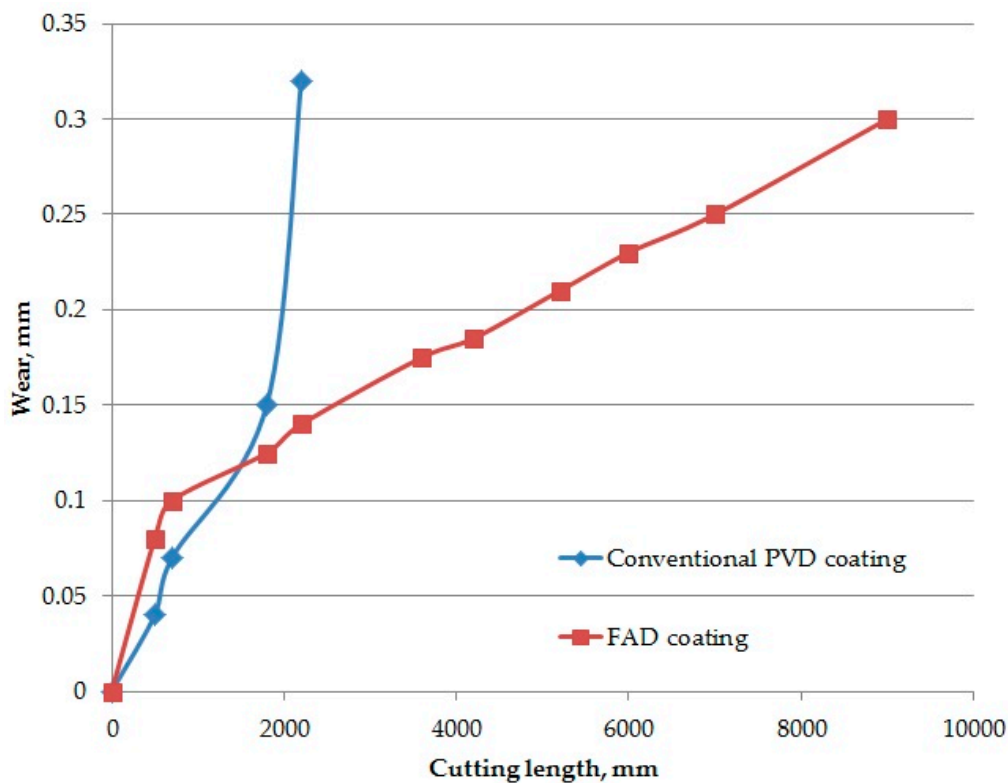


Figure 2. Dependence of mill coating wear on cutting length.

Table 2 shows that the properties of copper specimens quenched at different temperatures were similar. Moreover, Table 5 shows that coatings obtained by different technologies had the same microhardness. Thus, the materials had almost the same properties irrespective of the degree of non-equilibrium.

As can be seen in Table 6, Babbitt hardness and tensile strength increased with aging time. As a result, as the degree of nonequilibrium in the Babbitt grew, its hardness and tensile strength decreased.

Thus, the properties of the studied materials either did not change or improve as they approached the equilibrium state.

Table 2 shows that as the copper specimens moved away from the equilibrium state (increasing quenching temperature), electrical conductivity decreased. Consequently, thermal conductivity decreased as well. This is because increasing the quenching temperature leads to a corresponding increase in the content of vacancies. Point defects have the greatest effect on the electrical and thermal conductivity of metallic materials [18].

From Table 6, it follows that as the coating layer moved away from the equilibrium state (with the application of FAD technology), the grain size decreased and the number of crystal lattice defects grew. Just as in the copper samples, the thermal conductivity of the material decreased with distance from the equilibrium state. In addition, the friction coefficient diminished as the coating layer moved further from the equilibrium state.

From Table 7 it follows that hardness and wear rate decreased along with distance from the equilibrium state (reduction of the aging time), whereas tensile strength and scoring load become greater. A supersaturated lead-based solid solution decomposed during the aging of Babbitt. Magnesium, sodium, and calcium were released from the solid solution as a result of aging. Calcium in particular, formed an intermetallic compound CaPb_3 . Depletion of the solid solution led to an increase in the thermal conductivity of the alloy.

Tables 7 and 8 and Figure 2 show that for all materials, the wear rate decreased with distance from the equilibrium state. From Figure 2 it follows that in a nonequilibrium coating (FAD), self-organization

took place during friction at a point when wear rate showed a sharp decrease [13]. Following self-organization, the wear rate of the nonequilibrium coating (FAD) became less than that of the equilibrium coating (PVD). The opposite situation prevails prior to self-organization.

It was noted earlier that the production of entropy in non-equilibrium materials was greater than the production of entropy in relatively equilibrium ones under friction. Therefore, the wear rate of non-equilibrium materials must be greater than the wear rate of relatively equilibrium materials [11]. The wear rate of non-equilibrium materials may decrease due to self-organization. According to (6), an increase in the number of energy flows within a rubbing body increases the probability of self-organization. Consequently, relaxation processes increase the likelihood that self-organization will initiate.

Self-organization can take place only after the system loses its thermodynamic stability. Thermodynamic stability is determined by the sign of excess entropy production [14]. The entropy production of a rubbing body under friction according to [19] is the following:

$$\frac{ds_i}{dt} = X_h I_h = \frac{(kpv)^2}{\lambda T^2} \quad (7)$$

where: $I_h = -\lambda \text{grad}T = kpv$ —heat flow; $X_h = \frac{-\text{grad}T}{T^2}$ —thermodynamic force, inducing heat flow (k —friction coefficient, p —pressure, λ —heat conductivity coefficient, T —temperature, v —sliding speed).

According to [20], the system can lose its thermodynamic stability if the excess entropy production is negative:

$$\sum \delta X_h \delta I_h \leq 0 \quad (8)$$

The sum on the left-hand side of (8) is known as the excess entropy production. The values δX_h and δI_h are the respective deviations of the thermodynamic forces and flows from the steady state.

Let's presume that the degree of nonequilibrium in the friction material will affect its thermal conductivity and friction coefficient. To do this, we introduce the value ψ , which characterizes the deviation of the material from the equilibrium. In view of (7), the excess entropy production will be:

$$\sum \delta X_h \delta I_h = \delta(kpv) \delta \left(\frac{kpv}{\lambda T^2} \right) = \frac{(pv)^2}{T^2} \quad (9)$$

The right side of (9) can become negative if the second factor is negative. The condition for it is the following:

$$\frac{\partial k}{\partial \psi} \frac{\partial \lambda}{\partial \psi} > 0 \quad (10)$$

Condition (9) can be met if both the friction coefficient and thermal conductivity simultaneously increase or decrease when the friction material deviates from the equilibrium state.

As follows from the above data, a deviation from equilibrium leads to a simultaneous decrease in the friction coefficient and in thermal conductivity in all three materials studied. Therefore, non-equilibrium materials will have a lower wear rate compared to relatively equilibrium materials that are subject to condition (10). The comparative decrease in the wear rate of non-equilibrium materials is associated with the increased probability of self-organization when deviating from a state of equilibrium.

4. Conclusions

This study investigated three different materials (a sliding electrical contact (copper), a journal bearing (Babbitt) and a cutting tool coated with TiAlN) in nonequilibrium states of three different tribosystems. Results demonstrate that the wear rate of non-equilibrium materials was less than that

of equilibrium materials. The decrease in wear rate was associated with the greater likelihood of self-organization during friction in non-equilibrium materials.

Author Contributions: Conceptualization, I.G., and S.V.; methodology, I.G., E.I.G. and A.M.; validation, P.P., A.M. and E.K.; formal analysis, A.M.; investigation, P.P.; resources, E.K., and A.M.; data curation, E.K.; writing—original draft preparation, P.P.; writing—review and editing, I.G. and A.M.; visualization, P.P.; supervision, I.G. and A.M.; project administration, I.G. and E.K.

Funding: We would like to thank the Ministry of Science and Higher Education of the Russian Federation for supporting this work under the grant No. 14.574.21.0179 with unique identification number RFMEFI57417X0179.

Conflicts of Interest: The authors declare no conflicts of interest.

References

1. Klamecki, B.E. An entropy-based model of plastic deformation energy dissipation in sliding. *Wear* **1984**, *96*, 319–329. [[CrossRef](#)]
2. Klamecki, B.E. Energy dissipation in sliding. *Wear* **1982**, *77*, 115–128. [[CrossRef](#)]
3. Klamecki, B.E. Wear—An entropy production model. *Wear* **1980**, *58*, 325–330. [[CrossRef](#)]
4. Klamecki, B.E. A thermodynamic model of friction. *Wear* **1980**, *63*, 113–120. [[CrossRef](#)]
5. Bershadsky, I.I.; Iosebidse, D.S.; Kutelia, E.R. Tribosynthesis of graphite-diamond films and its employment structurally. *Thin Solid Films* **1991**, *204*, 275–293. [[CrossRef](#)]
6. Fox-Rabinovich, G.; Totten, G. *Advanced Surface-Engineered Materials and Systems Design*; Taylor & Francis Group: New York, NY, USA, 2006; p. 478, ISBN 1-57444-719-X.
7. Bryant, M.D. Entropy and dissipative processes of friction and wear. *FME Trans* **2009**, *37*, 55–607.
8. Nosonovsky, M. Entropy in tribology: In the search for application. *Entropy* **2010**, *12*, 1345–1390. [[CrossRef](#)]
9. Nosonovsky, M.; Mortazavi, V. *Friction-Induced Vibrations and Self-Organization: Mechanics and Non-Equilibrium Thermodynamics of Sliding Contact*; CRC Press: Boca Raton, FL, USA, 2013.
10. Nosonovsky, M.; Bhushan, B. Thermodynamics of surface degradation, self-organization and self-healing of biomimetic surfaces. *Philos. Trans. R. Soc. A* **2009**, *367*, 1607–1627. [[CrossRef](#)] [[PubMed](#)]
11. Gershman, I.S.; Bushe, N.A. Realization of dissipative self-organization on friction surface of tribosystems. *J. Frict. Wear* **1995**, *16*, 61–70.
12. Prigogine, I.; Konpeudi, D. *Modern Thermodynamics*; John Wiley & Sons: New York, NY, USA, 1999.
13. Gershman, I.S.; Gershman, E.I.; Mironov, A.E.; Fox-Rabinovich, G.S.; Veldhuis, S.C. Application of the Self-Organization Phenomenon in the Development of Wear Resistant Materials—A Review. *Entropy* **2016**, *18*, 385. [[CrossRef](#)]
14. Glansdorff, P.; Prigogine, I. *Thermodynamic Theory of Structure, Stability and Fluctuations*; Wiley Interscience: London, UK, 1970.
15. Fox-Rabinovich, G.S.; Gershman, I.S.; Yamamoto, K.; Bicsa, A.; Veldhuis, S.C.; Beake, B.D.; Kovalev, A.I. Self-Organization During Friction in Complex Surface Engineered Tribosystems. *Entropy* **2010**, *12*, 275–388. [[CrossRef](#)]
16. Amiri, M.; Khonsari, M.M. On the Thermodynamics of Friction and Wear—A Review. *Entropy* **2010**, *12*, 1021–1049. [[CrossRef](#)]
17. Fox-Rabinovich, G.S.; Weatherly, G.C.; Dodonov, A.I.; Kovalev, A.I.; Shuster, L.S.; Veldhuis, S.C.; Dosbaeva, G.K.; Wainstein, D.L.; Migranov, M.S. Nano-crystalline filtered arc deposited (FAD) TiAlN PVD coatings for high-speed machining applications. *Surf. Coat. Tech.* **2004**, *177–178*, 800–811. [[CrossRef](#)]
18. Cahn, R.W.; Haasen, P. *Physical Metallurgy*; North-Holland Physics Publishing: Amsterdam, The Netherlands, 1983.
19. Gershman, I.S.; Gershman, E.I.; Fox-Rabinovich, G.S.; Veldhuis, S.C. Description of Seizure Process for Gas Dynamic Spray of Metal Powders from Non-Equilibrium Thermodynamics Standpoint. *Entropy* **2016**, *18*, 315. [[CrossRef](#)]
20. Prigogine, I.; Nicolis, G. *Self-Organization in Nonequilibrium Systems*; Wiley: New York, NY, USA, 1977.

